Experimental Investigation of Precipitation-Static Dischargers in Wind

Claire Johnson, Benjamin C. Martell, Carmen Guerra-Garcia

MIT Department of Aeronautics and Astronautics

cnjohns@mit.edu, martellb@mit.edu, guerrac@mit.edu

Keywords: precipitation-static wicks, dischargers, wind tunnel, corona discharge, streamers in wind, self-pulsating discharge, electrostatics, aircraft

1. ABSTRACT

Aircraft and other airborne vehicles naturally acquire electrical charge during flight, due mainly to frictional charging by precipitation particles such as ice, snow, rain, or dust. If not properly managed using precipitation-static dischargers, or p-static wicks, corona discharges can form on the sharp edges of radio antennae, causing communication interference that impairs flight safety. The basic operation of these passive devices of charge control is explained by the onset of a controlled corona discharge at the tip of the wick whenever the aircraft acquires charge beyond the inception threshold of the discharge. Whereas testing standards are in place to quantify the charge dissipation rates of the wicks and their electromagnetic noise, these typically ignore aspects inherent to being airborne, such as sub-atmospheric pressure conditions or wind advection. In this work, wind tunnel experiments are conducted to characterize the behavior of corona discharge from commercial p-static wicks, mounted in standard testing configurations, subjected to DC voltage, and exposed to wind. The results from this experimental campaign reveal the effects of wind speed on the discharge properties, including which discharge mode is being favored (e.g., glow versus streamer corona), the streamer burst pulsation frequency, as well as current characteristics. These observations have implications in terms of the discharging efficiency of p-static wicks as well as their interference frequencies.

2. INTRODUCTION

Static dischargers are resistive devices used to silently dissipate the charge on an aircraft, limiting the charge build-up and controlling the electromagnetic interference of the discharge. Their function is therefore to bleed the charge from the aircraft at lower potential than it would naturally do, and with less noise. There are two types of static dischargers typically installed on aircraft, here referred to as (i) the horizontal-type, installed at trailing wing edges; and (ii) the angled-type, installed on tips of wings and stabilizers. Both types are slightly different but consist of a tip section, a resistive element, and a shank section for mounting [6]. Design considerations for aircraft p-static control and methods to verify adequate aircraft p-static performance can be found in the SAE standard ARP 5672 [6].

Laboratory tests on p-static wicks described by the Defense Standardization Program [1] and the Stanford Research Institute [2] are shown in Figure 1, and typically include measurement of discharge currents and electromagnetic noise. These tests are performed in static laboratory conditions, and therefore disregard the airborne environment (sub-atmospheric pressure) and the presence of wind. Typical diagnostics includes current and noise measurements at a range of DC voltage levels and for a fixed geometry. The wick is mounted vertically and spaced 6 inches above the ground plate. The ambient relative humidity and temperature are kept within the ranges of 40% to 60% and 16°C to 27°C, respectively, recognizing the important role that these parameters play in the gas discharge physics.

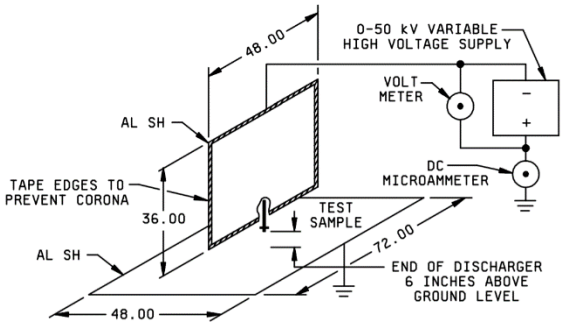

Fig 1. DOD discharge current test. Image taken from [1].

In particular, the discharge will be strongly dependent on the gas number density (through the lower gas pressures and temperatures encountered at altitude), and therefore scaling corrections are needed. E.g., to first order, the discharge inception electric field threshold is linear with the relative air density and the ion mobility scales inversely with relative air density [7]. In addition, wind effects will also play a role as they impact the transport of charged species, which in turn affects the electrostatics in the vicinity of the electrode [8]. When operating under DC fields, pulsating behavior can appear, and the frequency of these discharge pulsations is driven by the timescales of ion transport. Our recent work, using a simplified tip-to-plate electrode geometry, has shown that the frequency of streamer burst pulsations, their peak current magnitude, and the structure of the discharge is strongly influenced by wind [3], [4], [9].

In this study, we extend these academic studies to geometries of relevance to p-static wicks. We conduct a wind tunnel investigation to determine the effects of wind speed and applied voltage on the morphology of the discharge and regimes observed, as well as the electrical characteristics of the p-static wicks.

3. EXPERIMENTAL SETUP

A diagram of the experimental setup is shown in Figure 2 and a photograph is shown in Figure 3. A p-static wick is mounted on an insulating stand, downstream of a 46x46 cm open-return wind tunnel. A Matsusada RB60-30 DC high voltage power supply is used to apply varying voltages between 24kV and 30kV to the base of two separate Dayton-Granger p-static wicks, a null plus trailing edge discharger, which is typically mounted on the trailing edge of the wing, and a tip null plus discharger, which is mounted on the wing tip or the winglet. With respect to the wind direction, the trailing edge discharger is mounted at a 10 degree angle, while the tip discharger is mounted at a 45 degree angle. The wicks (including the retainer) are mounted to a plastic 3-d printed holder and centered with respect to the wind tunnel exit to minimize edge effects. Throughout this paper, the null plus trailing edge discharger will be referenced as the "horizontal wick" and the tip discharger as the "angled wick." The wicks have similar mechanical properties and are both made of a substrate coated with a high distributed resistance coating which carries the current on the outside of the wick. The angled wick has a shorter length than the horizontal wick. The electrical properties also slightly differ; the trailing edge discharger has a greater average resistance (6-200 MΩ vs. 6-120 MΩ) and greater RF discharge noise (approx. 36dB vs 30dB). Corresponding photographs of the wicks are shown in Figure 4.

A stainless-steel wire screen (mesh size 30x30 cm) is secured 15 cm downstream of the wick and connected to ground. The geometrical conditions of the test, such as the gap distance, are designed to match standard p-static wick testing protocols by the US DOD and other researchers [1,2].

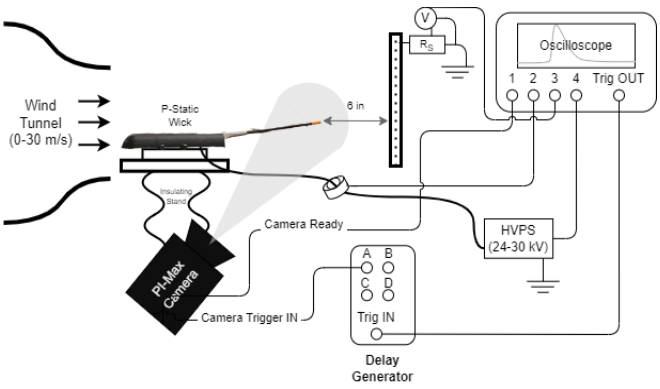

Fig 2. Schematic of the experimental setup for horizontal wick. The angled wick is not shown but is mounted the same way.

The ground-side current from the mesh screen is measured with a shunt resistor of 180 Ω and the time-resolved current at the high-voltage end is measured using a Pearson 2877 Rogowski coil. The voltage applied to the wick is measured with a time-resolved high-voltage probe (Lecroy PPE 20kV) to verify that the voltage did not vary significantly during streamer bursts.

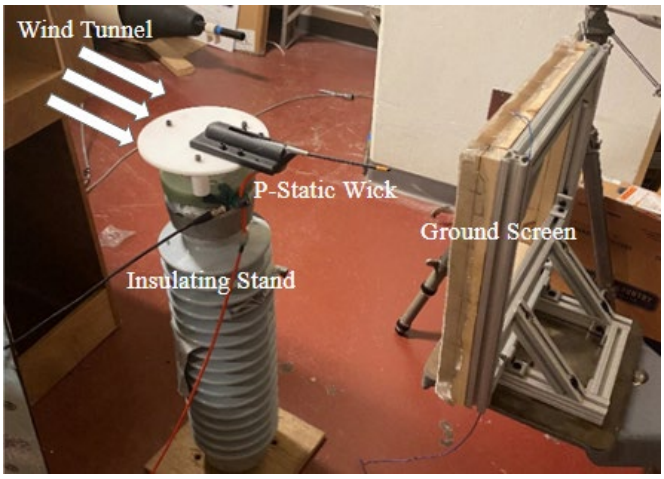

Fig 3. Image of testing setup with horizontal wick.

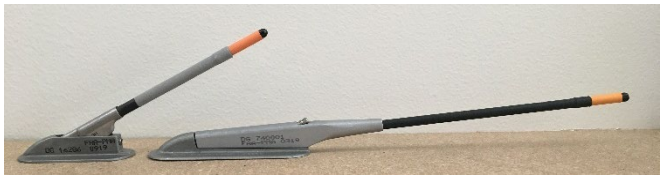

Fig 4. The two dischargers used for the study. Left is the tip null plus discharger mounted to the wing tip, referred to as the angled wick; Right is the null plus trailing edge discharger mounted to the trailing edge of the wing, referred to as the horizontal wick.

All electrical signals are measured by a WaveRunner 9000 Teledyne oscilloscope (4GHz bandwidth). For this study, the oscilloscope is set to collect $16 \cdot 10^6$ data points for each wind speed and voltage pairing. To accommodate variations in streamer pulse frequency, the collection time is set to 64 ms for all experiments except the 24 kV case, in which a larger sampling time of 160 ms was used, at the expense of a slightly lower sampling rate (100 MHz instead of 250 MHz). The sample period in this case, of 10 ns, is still well below the hundreds of nanoseconds pulse width, seen in Figure 5.

An example of the raw current waveforms can be seen in Figure 6a, for the case of horizontal wick at 28 kV applied voltage, and no wind. For this case, 110 pulses (above the noise level of around 50 μA) are recorded. Figure 5 shows those same pulse peaks aligned and overlaid, to visualize the consistent pulse shape and typical rise and fall times of individual pulses. The rise and fall times observed in this plot are consistent in characteristic time scale with previous experimentation done by our group [9]. The figure also demonstrates that the peak-finding algorithm used can properly identify the streamer burst pulsations despite the high level of noise.

Adding 30 m/s wind to the same wick at the same voltage makes the pulsating component of the discharge more infrequent and disperse in its properties, Figure 6b. Most notable is that the streamer pulsations become rarer and have a wider range of peak amplitudes: both with higher and lower amplitudes observed, compared to the no-wind baseline. The properties of the current pulses such as the inter-pulse period, peak current, and pulse width are analyzed statistically using distribution functions. These are presented in the results

section of the paper, Figures 10 through 15, and the analysis follows that presented in Ref [9]. The reader is referred to that paper for details on the statistical analysis and representation.

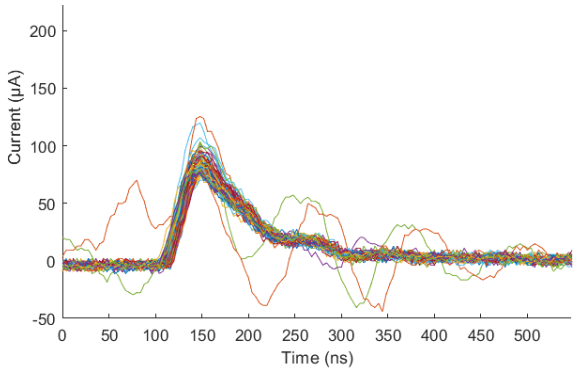

Fig 5. Overlaid pulses for 28 kV applied voltage and no wind on horizontal wick.

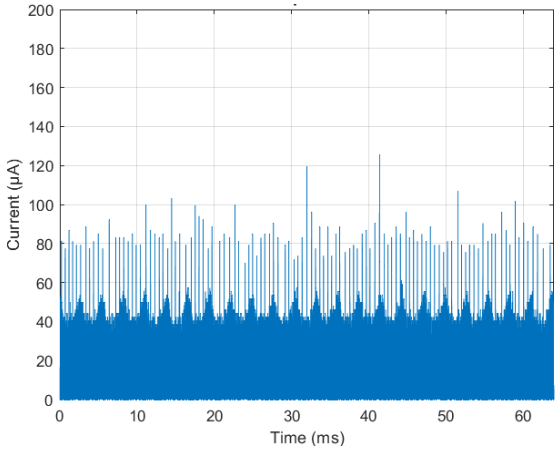

Fig 6a. Current time-traces for 28 kV applied voltage and no wind on horizontal wick.

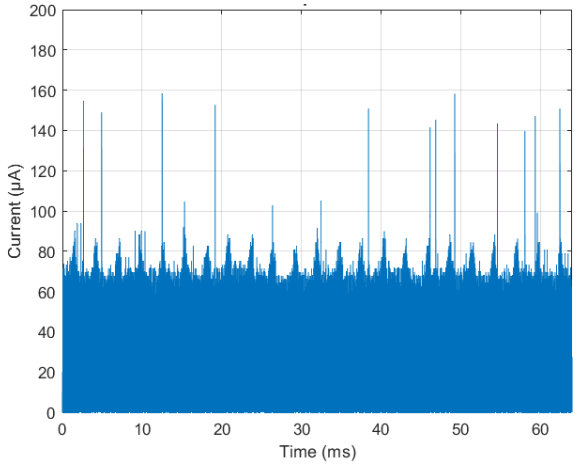

Fig 6b Current time-traces for 28 kV applied voltage and 30 m/s wind on horizontal wick.

A PIMAX-4 ICCD camera with a macro zoom lens (Vivitar Series 1 28-90mmm) pointed perpendicular to the flow, is used to image the corona discharge emitted from the tip of the discharger. To capture individual streamer bursts, the exposure time of the camera was varied between 0.5ms, 1ms and 2ms, with maximum gain. Figure 7 shows a sample of the imaging used in this work, including a single streamer burst, shown in a), and a superposition of 100 images of the discharge, shown in b).

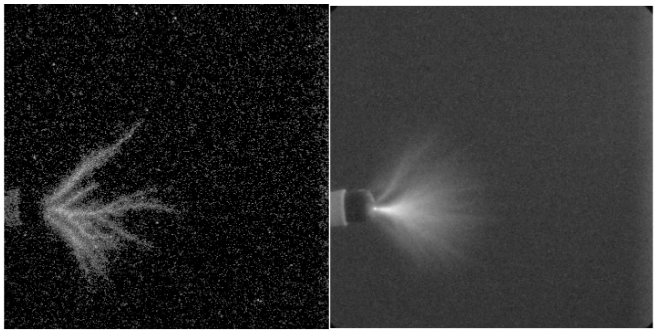

(a) (b)

Fig 7. (a) Single streamer burst and (b) multiple streamer bursts visualization using ICCD camera. Case of no wind and 24 kV.

4. RESULTS

Figures 8 and 9 show the visual appearance of the discharge, as a function of applied voltage and wind speed, through the superposition of 100 ICCD images. This visualization is therefore representative of what would be seen with the naked eye and not individual streamer bursts. The superposition is done in Matlab by averaging the intensity of the images for each pixel, normalized using the maximum value. Background noise is removed by identification of a noise threshold, to prevent misidentification of image superposition as glow discharge. In all these cases, two superimposed discharges can be observed: (i) a glow discharge, seen as a bright surface covering the head of the wick; and (ii) a streamer discharge, seen as a branching corona typically penetrating about 1 cm from the tip. For certain combinations of applied voltage and wind speed, the streamer discharge is infrequent and so most of the images capture a glow discharge. For other conditions, a more frequent appearance of streamer pulsations will allow more single burst images to be captured. The horizontal discharger results are shown in Figure 8 and the angled discharger results in Figure 9.

For the horizontal wick, the streamers emanating from the wick are a consistent size and shape in all the wind speeds and voltages tested. While the streamers visually look the same, they become much sparser as wind speed is added, and the glow discharge simultaneously brightens. A similar effect is observed at a fixed wind speed when the applied voltage is increased. Both higher wind and applied voltage stabilize the glow discharge and reduce the number of streamer bursts.

For the angled wick, the glow discharge similarly brightens with applied voltage and wind, but the frequency of streamer bursts seems to stay consistent. While the shape of the discharge remains constant throughout all horizontal wick tests, a change in shape is seen when the angled wick is subjected to high wind speeds; the streamers tilt slightly in upwind direction (e.g., the 30 kV, 30 m/s case shows the streamer stem location moving vertically upwards).

Figures 10 and 11 show the distribution functions for the inter-pulse period of streamer bursts at all the wind speeds and voltages tested, and the two wick configurations. The dark

histograms show the actual binned data, scaled relative to the global maximum of the full data set, so that all bins have equal weight. The lighter histograms are smoothed distributions and are all normalized to have the same maximum bin length for each distribution, to facilitate the visualization of the shape of the curve for regions that have fewer streamer bursts. The sparseness of some of the data can be seen here, for example the 30 kV (purple) case, in which only a few peaks were sampled in the fixed sample time. In the cases of very low frequency streamers (such as this dataset), it is difficult to capture high enough resolution current over time traces for confident pulse characteristics, while maintaining a high sample size, because the file size becomes too large to work with. Beginning with the no-wind case, a slight increase in pulsation frequency with voltage is observed, until 30 kV, where the discharge seems to be undergoing a transition to a stabilized glow regime (very few streamer bursts are captured).

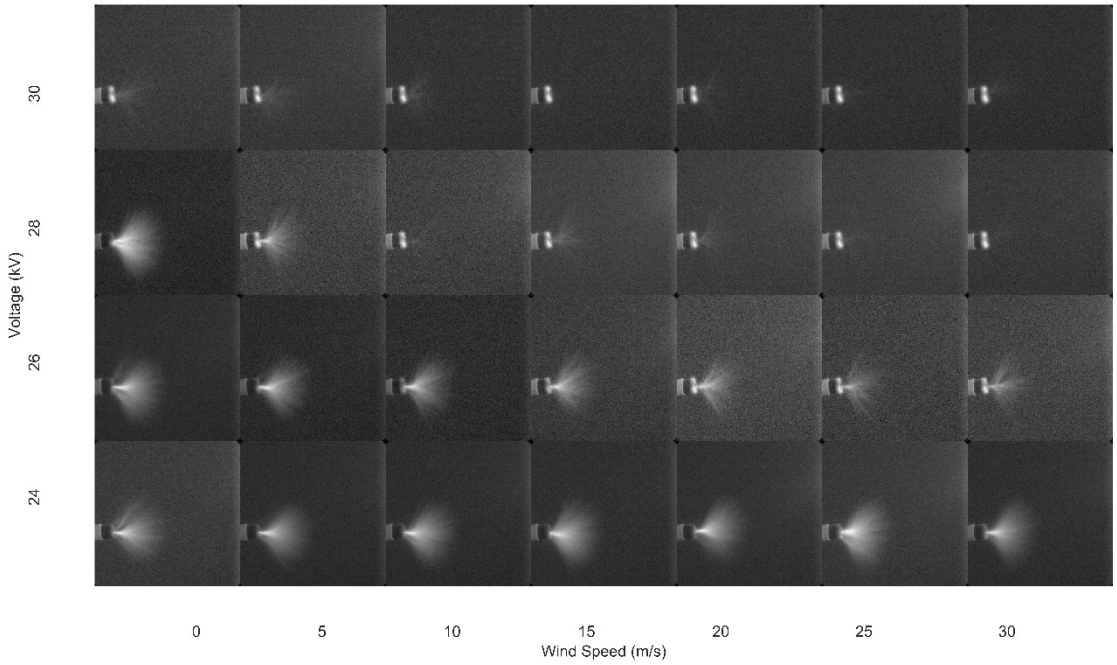

Fig 8. Time-integrated morphology of the discharge as a function of applied voltage and wind speed for the horizontally mounted discharger. Wind is going to the right.

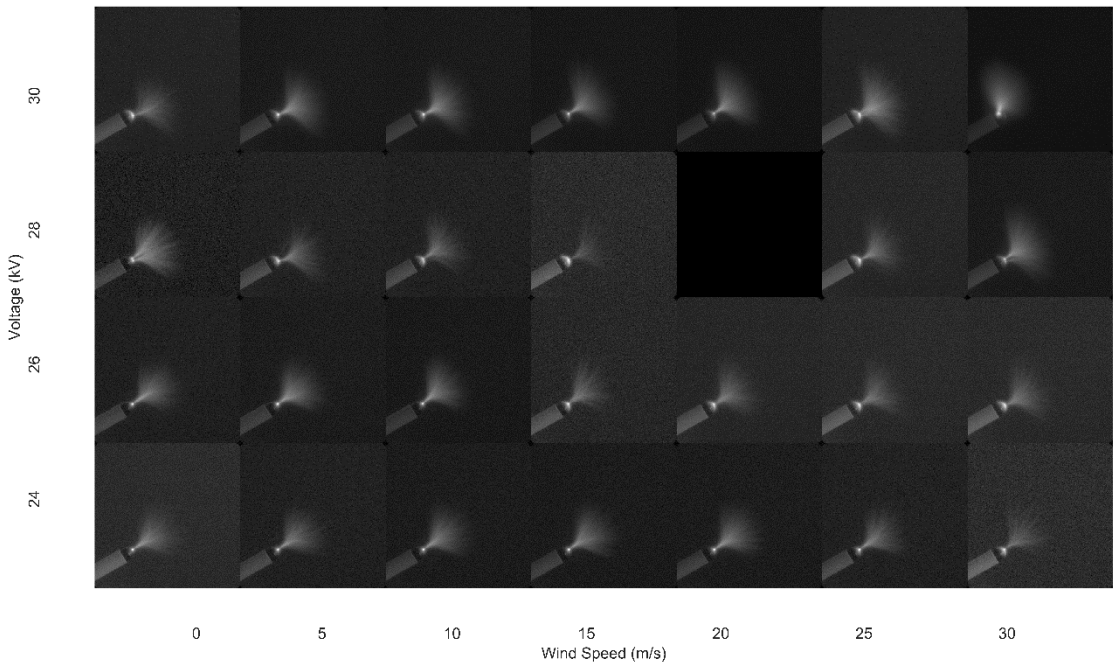

Fig 9. Time-integrated morphology of the discharge as a function of applied voltage and wind speed for the discharger mounted at a 45-degree angle to the wind. Wind is going to the right. Note the case of 28 kV, 20 m/s wind was missing data.

This observation aligns with the images in Figure 8. As wind speed is increased, there seems to be a small effect on the 24 kV case, but at 26 kV and 28 kV, an increase in dispersion and decrease in frequency is clear. This aligns with the glow becoming more prominent as the streamers become less prominent in the images of Figure 8. The 30 kV case was too low frequency to gather enough data for meaningful observations. The angled wick has similar trends, as seen in Figure 11. The 26 and 28 kV cases also get more disperse with wind speed. Interestingly, the 24 kV case and 30 kV cases seem to increase in frequency with wind speed, up to a point where they start to become more disperse again. The transition to vertically oriented streamers seen in the image of the 30 kV, 30 m/s case is not reflected in the waveforms.

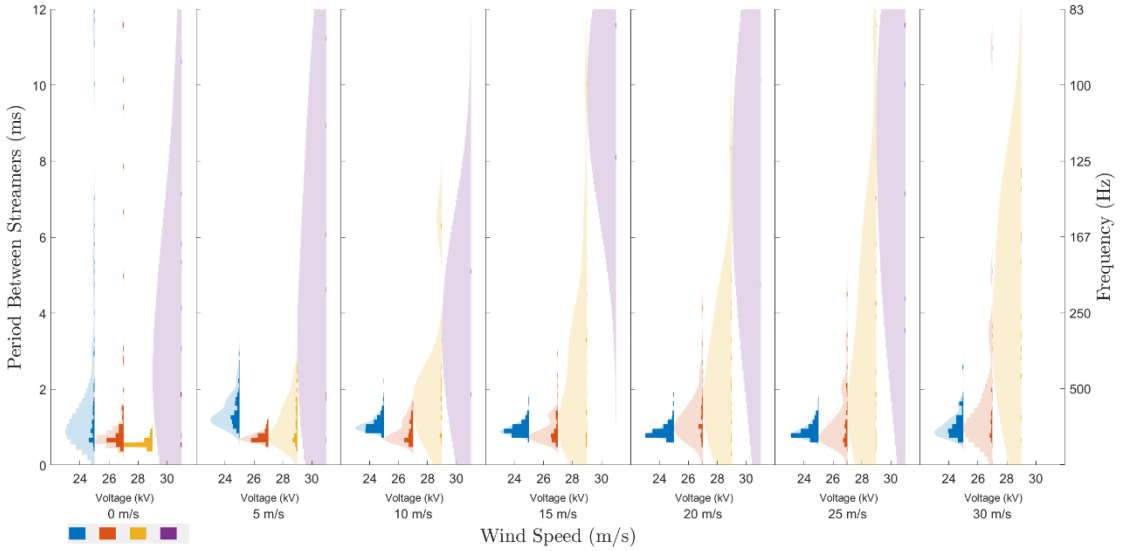

Fig 10. Effects of wind speed and voltage on inter-pulse period for the horizontal discharger.

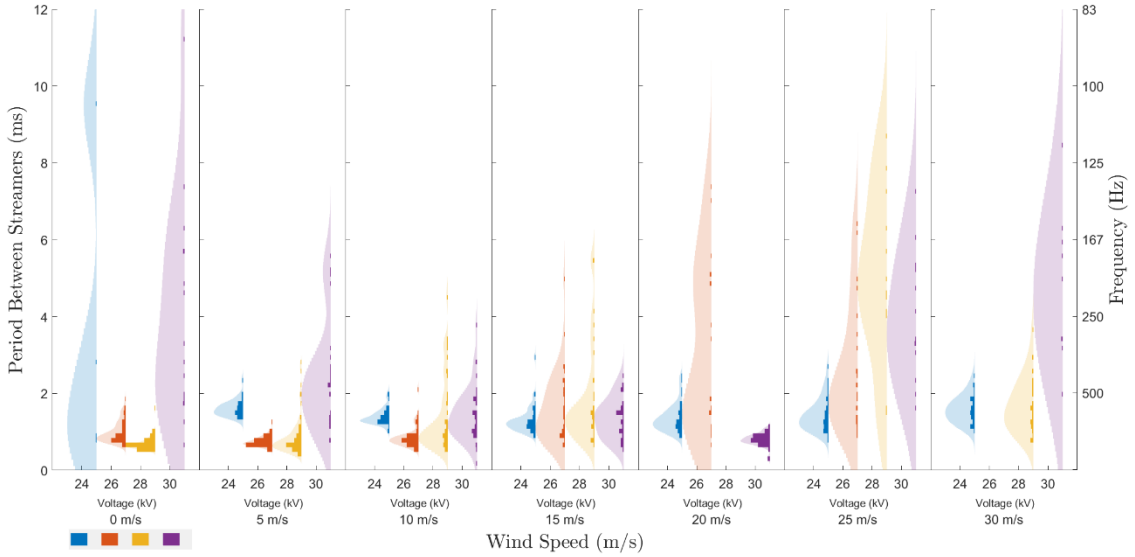

Fig 11. Effects of wind speed and voltage on inter-pulse period for the angled discharger. Note the cases of 28 kV, 20 m/s wind and 26 kV, 30 m/s wind were missing data.

The peak current of the streamer bursts is another interesting parameter to observe in terms of its distribution functions. This is shown in Figures 12 for the horizontal wick and 13 for the angled wick. Without wind, an increase in voltage results in a decrease in peak current, possibly associated to the higher frequency of the events. A transition at 30 kV to higher current streamers coincides with the regime transition to glow with very few streamer bursts observed in the imagery and inter-pulse period. When wind is added, the peak current tends to decrease slightly. The 28 kV applied voltage undergoes a

sharp transition at 15 kV from the lower current streamers to higher current streamers of similar magnitude to the 30 kV case. This coincides with the transition of 28 kV to be dominated by the glow discharge. Again, the angled wick has similar trends of decreasing peak current with wind speed and voltage, but with a significantly higher current. This is likely due to the inherent characteristics of the wicks themselves rather than their orientation. At some of the higher wind speeds and voltages tested, the peak current seems to start increasing, which may coincide with the streamers tilting vertically, as seen in the images of Figure 9.

The energy per pulse can be calculated by the time-integrated voltage times current. With a constant voltage, the energy matches the trends of the peak current, so has not been included for brevity. The typical energy for a 250 µA pulse would be 1 µJ for the 24 kV case. This calculation was done by integrating the current over the period of a single pulse and multiplying by the constant voltage.

The final parameter plotted is the pulse widths in figures 14 for the horizontal wick and 15 for the angled wick. This was calculated by taking the full width at half of the maximum (peak) current (FWHM). In most cases, for both the angled and horizontal wick, the widths do no change significantly with the addition of wind. The one exception is the 28 kV horizontal wick, which has a sharp increase simultaneous with the increase in current of Figure 12.

5. DISCUSSION

In contrast to previous works on idealized tip-to-plate geometries, the wind has less effect on the peak current and pulse widths. This finding is consistent with the lack of variation in streamer morphology throughout the imaging study. The parameter that changed the most with wind speed was the inter-pulse period, which along with the images indicate that the wind can have the effect of stabilizing a glow discharge and making streamer pulsations much sparser (for the range of parameters tested). The streamers become less frequent and less consistent with increasing voltage and wind speed. This effect may be due to the strengthening of the glow regime in the presence of wind. Seminal work on the influence of wind on glow corona discharge is due to S. Chapman and showed that the effect of the wind is to remove the shielding ions from the coronating tip vicinity, hence strengthening the glow [10,11]. The ion velocity in the absence of wind is the ion drift,

$$\boldsymbol{u}_{ion} = \mu\mathbf{E}. \tag{1}$$

With the addition of wind, the removal of ions is the superimposed velocity of the electric drift and the wind advection.

$$\boldsymbol{u}_{ion} = \mu\mathbf{E} + \boldsymbol{u}_{wind} \tag{2}$$

In atmospheric air and for positive polarity, the mobility µ is about 1.4 cm^2 /V/s [5], so for an average field of 2 kV/cm, the ion velocity is around 30 m/s. With wind at similar speeds, it will likely play a role in the removal of ions. By strengthening the glow, the streamer bursts become sparser and new locations for streamer inception might appear as the downstream side of the electrode is mostly affected by the advected ion cloud [12]. This study cannot speculate as to the difference between the inherent properties of the angled and horizontal dischargers since there are differences that are proprietary and unknown to the user.

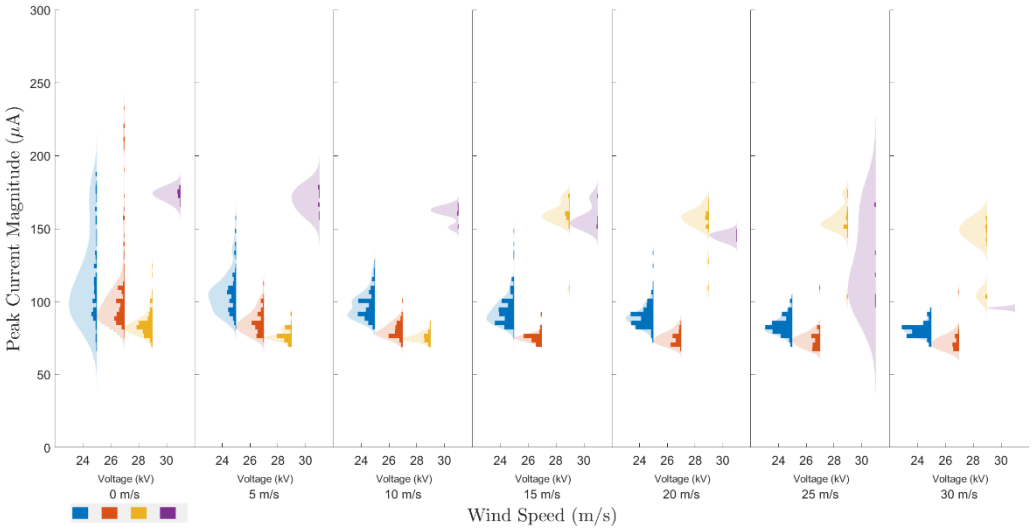

Fig 12. Effects of wind speed and voltage on peak current magnitude (horizontal wick).

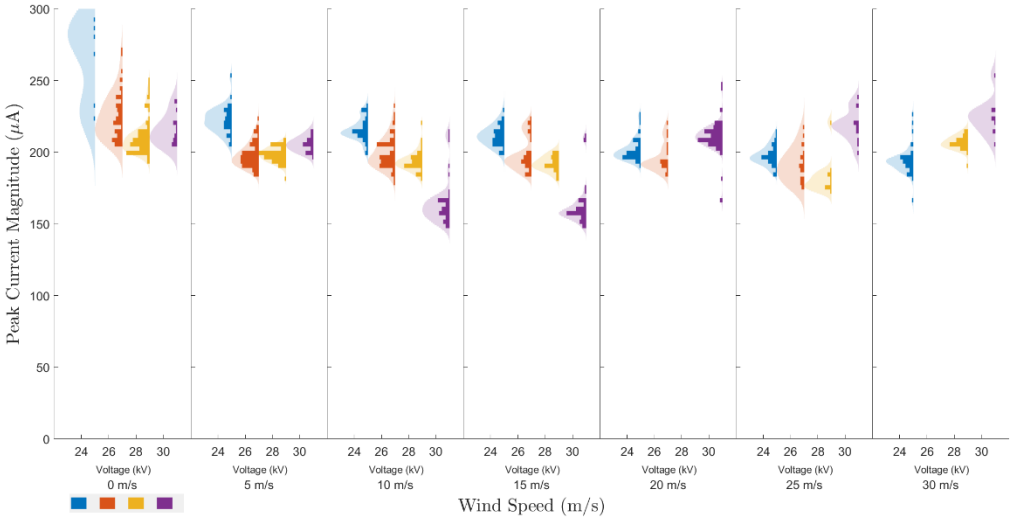

Fig 13. Effects of wind speed and voltage on peak current magnitude (angled wick).

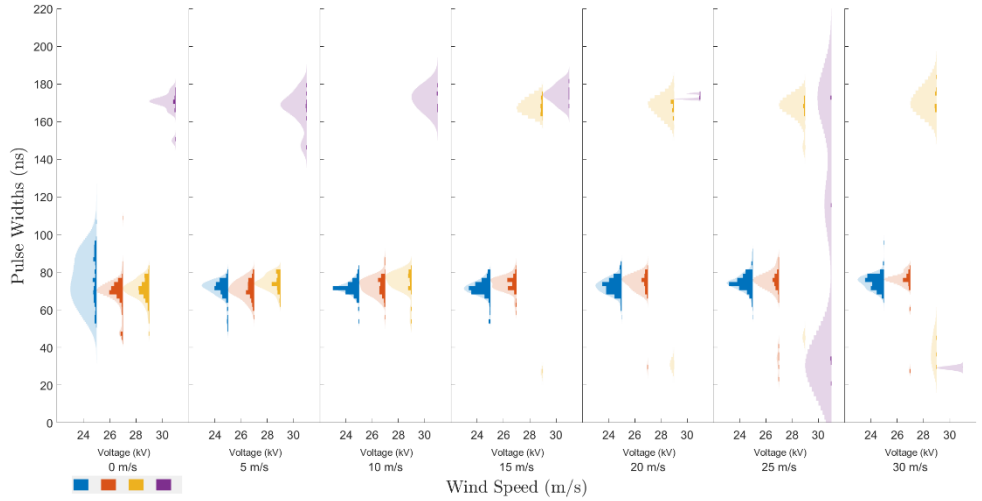

Fig 14. Effects of wind speed and voltage on pulse width (horizontal wick).

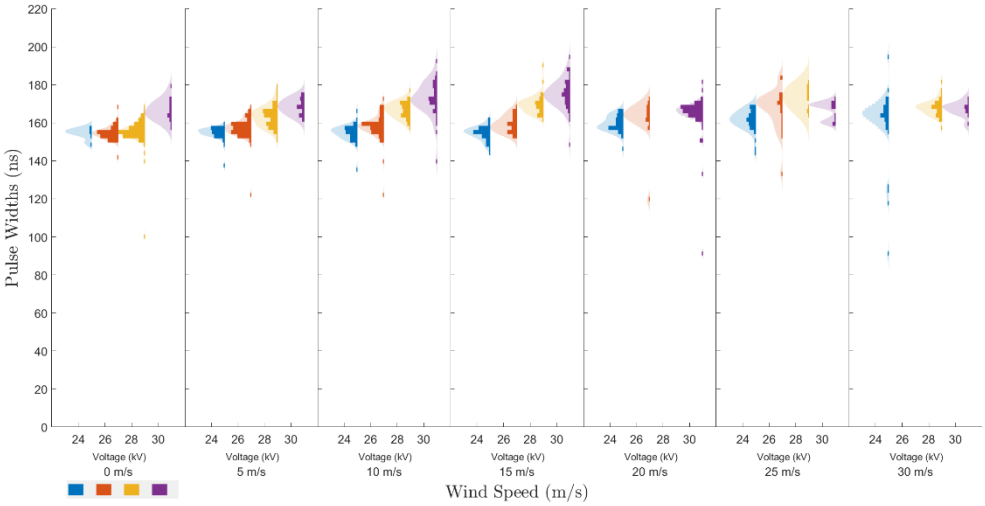

Fig 15. Effects of wind speed and voltage on pulse width (angled wick).

6. CONCLUSIONS

In this study we investigate the effects of wind and applied voltage on precipitation-static wick discharge properties. Two Dayton-Granger wicks, the tip null plus discharger and the null plus trailing edge discharger, were mounted in representative wind flow and both imaging and current waveform data were collected.

From the results of this study, we can conclude that increasing wind stabilizes p-static wick discharge by stimulating the transition from the streamer regime to a steadier DC glow around the tip. This stabilization is attributed to the enhanced ion transport and strengthening of the glow corona in response. As a result, the bursts become sparser, the frequency of pulsations decreases and there is more dispersion in the streamer properties, as voltage and wind speed increase. A slight decrease in peak current magnitude can also be observed although this trend does not hold for all tested voltages and thus cannot be generalized for all cases. The observations are specific to the testing configuration used and the range of voltages tested.

The results from this experimental campaign can have implications for future revisions of precipitation-static discharger military and FAA testing standards that currently do not include wind. Future experimentation could be conducted at higher wind speeds and higher voltages more conducive to airborne conditions, and this will be the focus of our future experiments.

ACKNOWLEDGEMENTS

We thank Christopher Maholm (Dayton-Granger) for providing both precipitation-static wicks and for useful discussions on the current industry testing processes of p-static wicks. We would also like to acknowledge the MIT Undergraduate Research Opportunities Program for facilitating this research partnership. The MIT team acknowledges partial support by The Boeing Company through the Strategic Universities for Boeing Research and Technology Program.

REFERENCES

[1] *United States Department of Defense, "Discharges, Electrostatic General Specification for. (Revision G Notice 1 - Validation)", 2019.*

[2] *R.L. Tanner. "Radio Interference from Corona Discharges", Technical Report, Stanford Research Institute, 1953.*

[3] *B.C. Martell, L.R. Strobel, A. Dogariu, C. Guerra-Garcia, "Self-pulsating streamer corona discharge under DC voltage", 74th Annual Gaseous Electronics Conference, online, 2021.*

[4] *B.C. Martell, L.R. Strobel, C. Guerra-Garcia, "Positive Streamer Corona Discharge Exposed to Wind", AIAA Aviation 2021 Forum, online, 2021.*

[5] *B. Zhang, J. He and Y. Ji, "IEEE Transactions on Dielectrics and Electrical Insulation", 24 923–929, 2017.*

[6] *SAE International, "Aircraft Precipitation Static Certification ARP5672", 2016.*

[7] *Y.P. Raizer, "Gas Discharge Physics (Berlin: Springer)", 1991.*

[8] *C. Guerra-Garcia, N.C. Nguyen, T. Mouratidis, M. Martinez-Sanchez, "Corona discharge in wind for electrically isolated electrodes." Journal of Geophysical Research: Atmospheres, 125, e2020JD032908, 2020.*

[9] *B.C. Martell, L.R. Strobel, C. Guerra-Garcia, "DC-driven positive streamer coronas in airflow", arXiv:2204.10947, 2022.*

[10] *S. Chapman, "Corona point current in wind", Journal of Geophysical Research, 75(12), 2165–2169, 1970.*

[11] *S. Chapman. "The magnitude of corona point discharge current", Journal of the Atmospheric Sciences, 34, 1801–1809, 1977.*

[12] *N.C Nguyen., C. Guerra-Garcia, J. Peraire, M. Martinez-Sanchez, "Computational study of glow corona discharge in wind: Biased conductor", Journal of Electrostatics, 89,1–12, 2017.*